Research Article | Vol. 9, No. 10 | 1 Oct 2018 | BIOMEDICAL OPTICS EXPRESS 4631
Biomedical Optics EXPRESS

Near-infrared fluorescence lymphatic imaging in vascular endothelial growth factor-C overexpressing murine melanoma

SUNKUK KWON,* FRED CHRISTIAN VELASQUEZ, AND EVA M. SEVICK-MURACA

Center for Molecular Imaging, The Brown Foundation Institute of Molecular Medicine, The University of Texas Health Science Center, Houston, TX 77030, USA
**sunkuk.kwon@uth.tmc.edu*

Abstract: In this study we employ a near-infrared fluorescence lymphatic imaging (NIRFLI) technique to longitudinally image spatial and temporal changes in the lymphatics in mice bearing vascular endothelial growth factor (VEGF)-C overexpressing B16F10 (VEGF-C-B16F10) or mock-transduced B16F10 (mock-B16F10) melanoma tumors. Our NIRFLI data show that ICG-laden lymph accumulates into a VEGF-C-B16F10 tumor compared to mock-B16F10 at 3 days post implantation, presumably due to increased lymphatic vessel permeability. Quantification shows a significantly greater percentage of ICG-perfused area in VEGF-C-B16F10 (7.6 ± 2) as compared to MOCK-B16F10 (1 ± 0.5; p = 0.02), which is also confirmed by quantification of the lymphatic leakage of evans blue dye (optical density at 610nm; VEGF-C-B16F10, 10.5 ± 2; mock-B16F10, 5.1 ± 0.5; p = 0.009); thereafter, lymphatic leakage is visualized only in the peritumoral region. Our imaging data also show that anti-VEGF-C treatment in VEGF-C-B16F10 restores normal lymphatic vessel integrity and reduces dye extravasation. Because NIRFLI technology can be used to non-invasively detect lymphatic changes associated with cancer, it may provide a new diagnostic to assess the lack of lymphatic vessel integrity that promotes lymphovascular invasion and to assess therapies that could arrest invasion through normalization of the lymphatic vasculature.

1. Introduction

Tumor-associated lymphatic vessel networks undergo significant changes in response to tumor cells, such as lymphatic vessel dilation and leakiness, and sprouting from pre-existing vessels [1,2]. These structural features of tumor lymphatic vessels might make them more susceptible for invasion by malignant cells, resulting in the increased probability of lymphatic metastasis [2]. One of the key lymphangiogenic factors for these changes is vascular endothelial growth factor (VEGF)-C, which has been shown to be critical for the proliferation of lymphatic endothelial cells (LECs) and initial lymphatic vessel sprouting [2].

VEGF-C binds to VEGF receptor (VEGFR)-3, which is predominantly expressed on lymphatic vessels [3]. Overexpression of VEGF-C in cancer cells induces tumor lymphangiogenesis and enhances tumor spread to the regional draining LNs in several mouse models of cancer [4]. Previous studies demonstrate that mice bearing VEGF-C overexpressing tumor show an increase in regional LN metastasis, retrograde lymph flow direction, and an increased number of dilated but functional peri-tumoral lymphatic vessels [5,6]. None of these studies provides longitudinal data showing when and how structural changes of the lymphatics occur in response to VEGF-C overexpressing tumor growth. Moreover, despite the importance of lymphatic vascular permeability in pathophysiological conditions [7], there are limited techniques to image lymphatic leakage due to enhanced permeability *in vivo*.

Recently, we developed non-invasive, dynamic near-infrared fluorescence lymphatic imaging (NIRFLI), and translated it within investigational studies in the clinic to examine lymphatic function of cancer patients and survivors using a microdose of fluorescent imaging

#335871 https://doi.org/10.1364/BOE.9.004631
Journal © 2018 Received 29 Jun 2018; revised 31 Jul 2018; accepted 10 Aug 2018; published 4 Sep 2018

Biomedical Optics EXPRESS

agent [8]. In this study, we investigate how VEGF-C impacts the lymphatics imaged by NIRFLI, longitudinally assessing the lymphatics in the hindlimb of mice where VEGF-C overexpressing B16F10 (VEGF-C-B16F10) or mock-transduced B16F10 (MOCK-B16F10) is implanted. Our data demonstrates that dynamic and longitudinal NIRFLI assessment of the lymphatic system may provide a companion diagnostic for therapies that seek to interrupt metastasis through arresting lymphangiogenesis.

2. Materials and methods

2.1 Cells and mice

VEGF-C- and mock-B16F10 cells were kindly provided by Dr. Timothy Padera at Massachusetts General Hospital and Harvard Medical School. To transfect VEGF-C- and MOCK-B16F10 cells expressing iRFP gene reporter (iRFP-VEGF-C-B16F10 and iRFP-MOCK-B16F10, respectively), cells were cultured as monolayer in DMEM-F12/10% fetal bovine serum (FBS, BioExpress, Kaysville, UT, USA). At near confluency, the culture was transfected with piRFP plasmid (Addgene, Cambridge, MA, USA) by Lipofectamine 2000 (Invitrogen, Grand Island, NY, USA) as suggested by the manufacturer. Transfected cells were grown under 0.8 mg/ml G418 selection in DMEM-F12/10% FBS growing medium. Transfected cells that survived the antibiotic selection were then sorted through flow cytometry outfitted with 690 nm/730 nm (excitation/emission) wavelengths to obtain the population of high iRFP expressers.

Six to eight week old female C57BL6 mice (Charles River, Wilmington, MA) were housed and fed sterilized pelleted food and sterilized water at the Brown Foundation Institute of Molecular Medicine at the University of Texas Health Science Center – Houston (UTHSC-H). All experiments were performed in accordance with the guidelines of the Institutional Animal Care and Use Committee of UTHSC-H.

2.2 Blocking antibody and treatment

A neutralizing rat monoclonal antibody specific for mouse VEGFR-3 (n = 6; mF4-31C1; 800 µg/mouse; ImClone Systems Inc., New York, NY) or control rat IgG (n = 5; 800 µg/mouse; Antibodies incorporated, Davis, CA) was administered at the time of tumor cell injection and every second day.

2.3 In vivo fluorescence imaging

Mice were imaged for baseline information with i.d. injection of 10 µl of 645 µM of ICG (Akorn, Inc. Buffalo Grove, IL) using 31 gauge needles (BD Ultra-FineTM II Short Needle, Becton and Dickinson Medical, Franklin, NJ). After baseline imaging, iRFP expressing or non-expressing VEGF-C- or mock-B16F10 cells (5 x 10^5) in 10 µl PBS were inoculated intradermally into the left hindlimb and thereafter, tumor volume was longitudinally measured using a digital caliper. Tumor volume (mm^3) was calculated using the following formula: 0.52 x $D1^2$ x D2, where D1 and D2 are short and long tumor diameters, respectively. NIRFLI with i.d. injection of 10ul of ICG was performed longitudinally at 3, 7, and 10 days post tumor implantation (p.i.). Therefore, mice were injected four times with ICG (at baseline, and day 3, 7, and 10). In addition, in order to explore whether increased vessel permeability seen with ICG was evident with high MW vascular agents known not to extravasate from intact vasculatures, a subset of mice (n = 2) were injected with 10 µl (10 mg/ml) of FITC-Dextran (2M Da; Sigma) several millimeters proximally away from the ICG injection site at 3 days p.i.. For imaging FITC-Dextran, an Argon-Krypton laser system (50mW, 488nm) was used to illuminate mice. Bandpass (510nm center wavelength) and holographic filters (488nm center wavelength) were used to collect re-emitted fluorescence light and reject the excitation light, respectively. A series of sequential NIRF and FITC-Dextran images were acquired with 200ms exposure time immediately before and for up to 20 min after i.d. injection. NIRF and

Biomedical Optics EXPRESS

iRFP images were acquired using a custom-built imaging system described elsewhere [9,10]. A macrolens (Infinity K2/SC video lens, Edmund Optics Inc., Barrington, NJ) was also used to zoom in on a specific area in fluorescent lymphatic vessels. For all procedures, mice were anesthetized with isofluorane and maintained at 37 °C on a warming pad.

2.4 Measurement of lymphatic vascular leakage and perfused area analysis

Two µl of Evans blue dye (EBD; 3% by weight) was injected intradermally at the base of the tail 3 days after VEGF-C (n = 6) or MOCK (n = 5) B16F10 inoculation. Twenty minutes after injection, animals were euthanized and tumors collected, weighed, and incubated for 48 hrs in 1 ml of formamide at 60°C to extract EBD from the tissue. The optical density at 610 nm (OD610; absorption) was measured for each sample using spectrophotometer.

The percentage of the perfused area from NIRFLI was calculated using ImageJ. In addition, a fixed region of interest (ROI) was defined in the tumor on sequential frames of fluorescence images. The mean of the fluorescence intensity within the ROI in each fluorescence image was calculated and then plotted as a function of imaging time.

2.5 Statistics

Data were presented as average values ± standard error (SE). Statistical analysis was performed with Prism 5 (Graphpad Software, Inc). The data were tested for normality using a D'Agostino and Pearson Omnibus normality test prior to analysis. The Mann-Whitney test was used for comparisons between two groups or Kruskal–Wallis test with Dunn's multiple comparisons test was used. The significance level is set as $p < 0.05$.

3. Results

3.1 VEGF-C overexpression results in leakage of ICG-laden lymph into VEGF-C-B16F10 at early post implantation

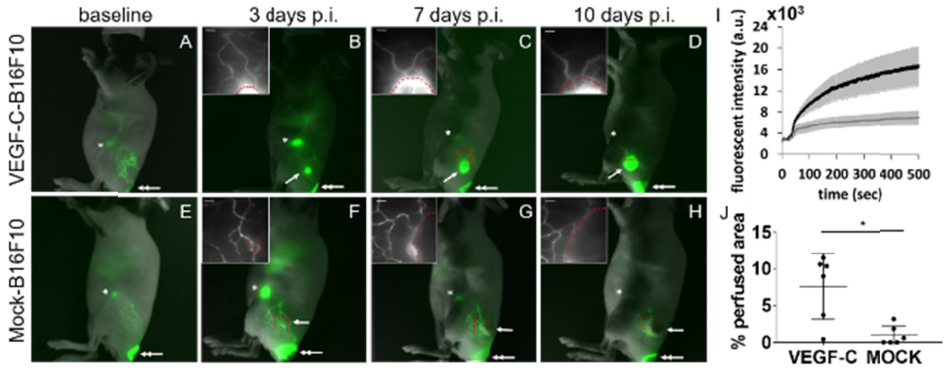

Fig. 1. Representative fused images of fluorescence with white light images in mice bearing VEGF-C or MOCK-B16F10 in the left hindlimb. NIRFLI showed dye accumulation in the tumor after ICG administration (See Visualization 1). The insets show magnified fluorescent images of the red rectangles. A dashed red circle in the inset indicates the location of a tumor. Arrow, tumor. Double arrow, ICG injection site. Asterisk, ILN. Scale, 1mm. I. The fluorescent intensity profiles in the VEGF-C- (n = 6; black) and MOCK- (n = 6; grey) B16F10 tumor region at 3 days p.i. were plotted as a function of time. Data was shown mean ± SE. J. Quantification showing percentage of ICG perfused area in VEGF-C (n = 6) and MOCK- (n = 6) B16F10. * P = 0.02.

Using non-invasive, dynamic NIRFLI immediately following i.d. injection of ICG to the base of the tail, different lymphatic drainage networks are shown in the hind limb of each mouse draining the base of the tail into the inguinal LN (ILN), which is connected to the axillary LNs (ALNs) through internodal collecting lymphatic vessels (Fig. 1). To explore the temporal nature of lymphatic changes, we longitudinally imaged mice from 3 days after inoculation of

Biomedical Optics EXPRESS

VEGF-C-B16F10 or mock-B16F10. Dynamic NIRFLI at 3 days p.i. of tumor cells revealed extravasation of ICG tracer into VEGF-C-B16F10 as evidenced by strong ICG fluorescence in the tumor (arrow in Fig. 1(B)) and the fluorescent intensity profiles in the tumor over time (Fig. 1(I)). We observed this feature in all VEGF-C-B16F10 bearing mice where fluorescent lymphatic vessels pass through the tumor after i.d. injection to the base of the tail. ICG-laden lymph leaked out of lymphatic vessels at the tumor margin and diffused into the tumor as shown in Visualization 1. Magnified fluorescent images showed that VEGF-C-B16F10 draining lymphatic vessels gradually dilated during tumor progression (insets in Figs. 1(B) – 1(D)). In contrast, we could not observe extravasation of ICG into mock-B16F10 as seen in VEGF-C-B16F10. ICG-laden lymph drained along the lymphatic vessels in the skin above mock-B16F10 at 3 days p.i. (Fig. 1(F)) and stained around the tumor margin at later time points (Figs. 1(G) and 1(H)). Quantification of the perfused area shows a significant difference between VEGF-C- and MOCK-B16F10 (Fig. 1(J)). Lymphatic permeability assay showed significant leakage of EBD in VEGF-C-B16F10 as compared to MOCK-B16F10 (Fig. 2(A)), confirming the *in vivo* imaging data shown in Fig. 1. There was no significant difference in tumor growth rate between VEGF-C- and mock-B16F10 (Fig. 2(B)).

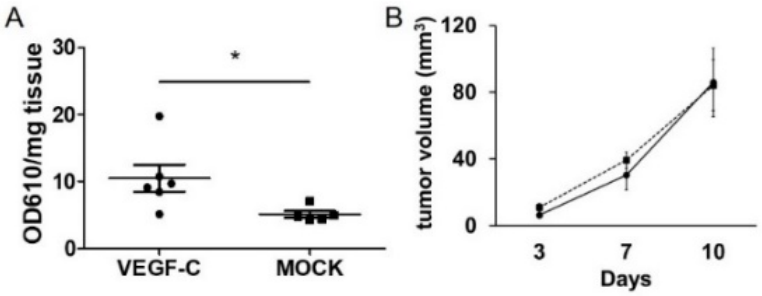

Fig. 2. A. Quantification of tissue retention of EBD normalized to tissue weight. * p = 0.009. B. In vivo growth of VEGF-C-B16F10 (circle; n = 8) and MOCK-B16F10 (square; n = 11).

3.2 VEGF-C overexpression also results in leakage of high molecular weight FITC-Dextran into VEGF-C-B16F10 at early post implantation

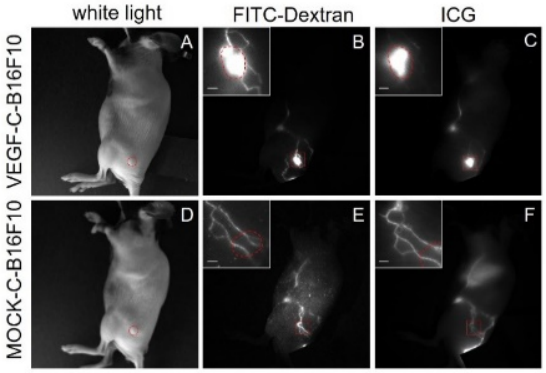

Fig. 3. White and fluorescence images in mice (n = 2 for each tumor) at 3 days p.i. of VEGF-C or MOCK-B16F10 following FITC-Dextran and ICG. The insets show magnified fluorescent images of the red rectangles. A dashed red circle in the inset indicates the location of a tumor. The injection sites were covered. Scale, 1mm.

Molecular weight can be a key factor in extravascular distribution out of the leaky lymphatic vessels. Therefore, we tested if lymphatic vessel leakage as shown from ICG in Fig. 1 is still observed using the high molecular weight FITC-Dextran (MW 2,000 KDa), which is largely

Biomedical Optics EXPRESS

retained by intact blood vasculature [11]. FITC-dextran stained patterns of lymphatic vessel networks similar to that observed with ICG fluorescence (Fig. 3). We observed the leakage of FITC-dextran into VEGF-C-B16F10, but not into mock-B16F10 at 3 days p.i. (Fig. 3).

3.3 Anti-VEGFR-3 treatment restores normal lymph flow drainage patterns

We next tested if NIRFI can image the ability of VEGFR-3 blockade to reverse altered lymphatic drainage patterns. To this end, a rat monoclonal antibody to murine VEGFR-3, mF4-31C1 [12], was injected intraperitoneally beginning the day of implantation of VEGF-C-B16F10 tumor cells. NIRFI data showed that extravasation of ICG-laden lymph into the tumor due to VEGF-C- overexpression was significantly reduced by anti-VEGFR-3 treatment as compared to control IgG (Fig. 4(B)).

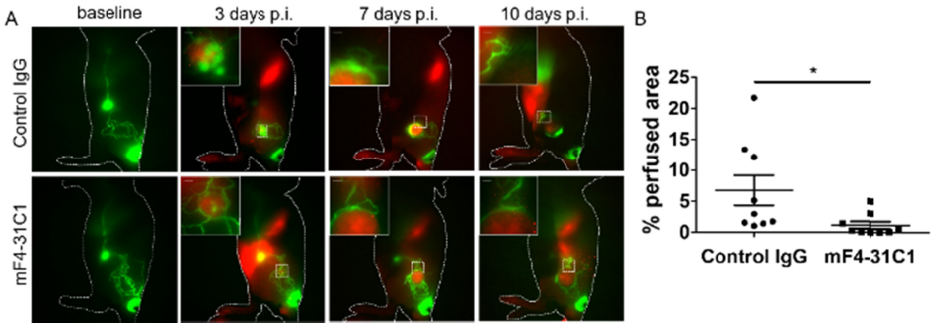

Fig. 4. A. Representative *in vivo* fluorescence images of mice at 3 days p.i. of iRFP-VEGF-C-B16F10 (red; n = 9 for each treatment) 20 mins after i.d. injection of ICG (green) to the base of the tail. The insets show magnified fluorescent images of the white dashed rectangles. For comparison of mock-B16F10, see Fig. 1. B. Quantification showing percentage of ICG perfused area in the tumor region. * P = 0.001. Scale, 1mm.

4. Discussion

The lymphatic system provides a major route of cancer cell dissemination from the primary lesion site to regional draining LNs. A consequence of complex multistep processes is required to develop LN metastasis, including the dissemination of tumor cells from the primary tumor site by invading pre-existing or lymphangiogenic lymphatic vessels [1,2]. Lymphangiogenic growth factor VEGF-C induces increased formation of tumor-directed lymphatic vessel sprouts with open lumen structure, enveloping tumor cells, and dilation of peri-tumor lymphatic vessels [5,13,14]. Non-invasive imaging of tumor-associated lymphatics has been used to show that these tumor-associated lymphatic vessels are tortuous, leaky, and highly disorganized [5,6,13,14]. However, most tumors in past studies were located in the ear or tail, where visual observation was directly made following intra/peritumoral injection. More importantly these imaging studies were performed at one time point and did not show the dynamic aspects of lymphatic structural plasticity. In this study, we non-invasively imaged dramatic changes of tumor-associated lymphatic architecture during VEGF-C or MOCK-B16F10 tumor progression, including significant extravasation of ICG and FITC-dextran from disrupted pre-existing lymphatic vessels around the tumor at early stages and gradual dilation of tumor-draining lymphatic vessels over time in response to excess VEGF-C, which were not observed in mock-B16F10 and baseline imaging. Previous studies to measure the permeability of isolated normal lymphatic vessels showed that small molecular hydrophilic substances less than 4 kDa are permeable from the intraluminal to extraluminal space of lymph vessels. ICG binds to plasma proteins, among which albumin is the prevalent protein in the interstitial space. Therefore, if one considers that intradermally injected ICG binds to albumin, the effective molecular weight of ICG-albumin binding reaches 67 kDa. The ICG leakage presented in this study may be not due to its low

Biomedical Optics EXPRESS

molecular weight, since we also observed extravasation of 2000 kDa FITC-Dextran. FITC-Dextran has been used for fluorescence microlymphangiography (FML) in tumor-associated lymphatics [5]. Although FML is useful to understand changes in lymphatic capillaries and cutaneous lymphatic vessels, clinical application is limited owing to the limited penetration depth of light at visible wavelengths and tissue scattering, and the inability to visualize deeper collecting and conducting lymphatic vessels.

We show that ICG leakage in VEGF-C expressing tumors occurred at early stages (Fig. 1). When solid tumors grow, interstitial fluid pressure (IFP) is elevated compared with normal tissues due to mechanical stress generated by tumor cell growth [15]. Although we did not measure IFP at 3 days p.i. (as small as 8 mm^3 in tumor volume), previous data showed that IFP in VEGF-C overexpressing tumors is higher than that in normal tissues, but similar to that in control tumors [5]. Therefore, extravasation of ICG-laden lymph in early stage VEGF-C-B16F10 tumors presented in this study may be due to destabilization of the lymphatic vessel wall by tumor-secreted VEGF-C, while anti-VEGFR-3 treatment significantly normalized these vessels.

In conclusion, we demonstrated our ability to image architectural changes of tumor-associated lymphatics in vivo during tumor progression with i.d. injection of ICG. Increasing the permeability of the lymphatic vasculature is one of the hallmarks of cancer and inflammation. Therefore, a better understanding of changes to lymphatic structure and drainage patterns in disease may provide new strategies to improve drug exposure to targets in the lymphatic system and enhance therapeutic utility. Since technology is already used within investigational studies in the clinic to image the lymphatic system longitudinally [16], NIRFLI may also provide information in lymphatic response to anti-VEGF-C and other therapies.

Funding

National Institutes of Health (R21CA159293).

Acknowledgments

We would like to acknowledge Dr. Timothy Padera at Massachusetts General Hospital and Harvard Medical School for kindly providing VEGF-C- and mock-B16F10. This work was supported by the National Institutes of Health R21CA159293. We thank Dr. Germaine Agollah and Grace Wu for their technical assistance and Dr. Wenyaw Chan for assistance of statistical analysis. We also thank Dr. Bronislaw Pytowski (Oncologie, Inc) for generously providing the mF4-31C1 antibody.

Disclosures

The authors declare that there are no conflicts of interest related to this article.

References

1. S. A. Stacker, M. G. Achen, L. Jussila, M. E. Baldwin, and K. Alitalo, "Lymphangiogenesis and cancer metastasis," Nat. Rev. Cancer **2**(8), 573–583 (2002).
2. A. Alitalo and M. Detmar, "Interaction of tumor cells and lymphatic vessels in cancer progression," Oncogene **31**(42), 4499–4508 (2012).
3. V. Joukov, K. Pajusola, A. Kaipainen, D. Chilov, I. Lahtinen, E. Kukk, O. Saksela, N. Kalkkinen, and K. Alitalo, "A novel vascular endothelial growth factor, VEGF-C, is a ligand for the Flt4 (VEGFR-3) and KDR (VEGFR-2) receptor tyrosine kinases," EMBO J. **15**(7), 1751 (1996).
4. J. L. Su, C. J. Yen, P. S. Chen, S. E. Chuang, C. C. Hong, I. H. Kuo, H. Y. Chen, M. C. Hung, and M. L. Kuo, "The role of the VEGF-C/VEGFR-3 axis in cancer progression," Br. J. Cancer **96**(4), 541–545 (2007).
5. T. P. Padera, A. Kadambi, E. di Tomaso, C. M. Carreira, E. B. Brown, Y. Boucher, N. C. Choi, D. Mathisen, J. Wain, E. J. Mark, L. L. Munn, and R. K. Jain, "Lymphatic metastasis in the absence of functional intratumor lymphatics," Science **296**(5574), 1883–1886 (2002).
6. N. Isaka, T. P. Padera, J. Hagendoorn, D. Fukumura, and R. K. Jain, "Peritumor lymphatics induced by vascular endothelial growth factor-C exhibit abnormal function," Cancer Res. **64**(13), 4400–4404 (2004).

Biomedical Optics EXPRESS

7. S. Liao and P. Y. von der Weid, "Inflammation-induced lymphangiogenesis and lymphatic dysfunction," Angiogenesis **17**(2), 325–334 (2014).
8. E. M. Sevick-Muraca, S. Kwon, and J. C. Rasmussen, "Emerging lymphatic imaging technologies for mouse and man," J. Clin. Invest. **124**(3), 905–914 (2014).
9. S. Kwon and E. M. Sevick-Muraca, "Functional lymphatic imaging in tumor-bearing mice," J. Immunol. Methods **360**(1-2), 167–172 (2010).
10. B. Zhu, H. Robinson, S. Zhang, G. Wu, and E. M. Sevick-Muraca, "Longitudinal far red gene-reporter imaging of cancer metastasis in preclinical models: a tool for accelerating drug discovery," Biomed. Opt. Express **6**(9), 3346–3351 (2015).
11. M. R. Dreher, W. Liu, C. R. Michelich, M. W. Dewhirst, F. Yuan, and A. Chilkoti, "Tumor vascular permeability, accumulation, and penetration of macromolecular drug carriers," J. Natl. Cancer Inst. **98**(5), 335–344 (2006).
12. B. Pytowski, J. Goldman, K. Persaud, Y. Wu, L. Witte, D. J. Hicklin, M. Skobe, K. C. Boardman, and M. A. Swartz, "Complete and specific inhibition of adult lymphatic regeneration by a novel VEGFR-3 neutralizing antibody," J. Natl. Cancer Inst. **97**(1), 14–21 (2005).
13. T. Hoshida, N. Isaka, J. Hagendoorn, E. di Tomaso, Y. L. Chen, B. Pytowski, D. Fukumura, T. P. Padera, and R. K. Jain, "Imaging steps of lymphatic metastasis reveals that vascular endothelial growth factor-C increases metastasis by increasing delivery of cancer cells to lymph nodes: therapeutic implications," Cancer Res. **66**(16), 8065–8075 (2006).
14. Y. He, I. Rajantie, K. Pajusola, M. Jeltsch, T. Holopainen, S. Yla-Herttuala, T. Harding, K. Jooss, T. Takahashi, and K. Alitalo, "Vascular endothelial cell growth factor receptor 3-mediated activation of lymphatic endothelium is crucial for tumor cell entry and spread via lymphatic vessels," Cancer Res. **65**(11), 4739–4746 (2005).
15. G. Baronzio, G. Parmar, and M. Baronzio, "overview of methods for overcoming hindrance to drug delivery to tumors, with special attention to tumor interstitial fluid," Front. Oncol. **5** 165 (2015).
16. J. C. Rasmussen, I. C. Tan, S. Naqvi, M. B. Aldrich, E. A. Maus, A. I. Blanco, R. J. Karni, and E. M. Sevick-Muraca, "Longitudinal monitoring of the head and neck lymphatics in response to surgery and radiation," Head Neck **39**(6), 1177–1188 (2017).